

Structure–property relations in individual carbon nanotubes [Invited]

FENGRUI YAO,¹ JINGYI TANG,¹ FENG WANG,^{2,3,4} AND KAIHUI LIU^{1,5}

¹State Key Laboratory for Mesoscopic Physics, Center for Nanochemistry, Collaborative Innovation Center of Quantum Matter, School of Physics, Peking University, Beijing 100871, China

²Department of Physics, University of California at Berkeley, Berkeley, California 94720, USA

³Advanced Light Source Division and Materials Sciences Division, Lawrence Berkeley National Laboratory, Berkeley, California 94720, USA

⁴e-mail: fengwang76@berkeley.edu

⁵e-mail: khliu@pku.edu.cn

Received 11 February 2016; revised 10 April 2016; accepted 26 April 2016; posted 28 April 2016 (Doc. ID 259219); published 20 May 2016

After more than a quarter century's intense research and exploration for their distinctive physical properties and potential applications, carbon nanotubes remain an active research field with many surprises and opportunities. Recent advances in nano-optics provide a powerful tool to optically characterize carbon nanotubes with a defined chiral index at the single-nanotube level. Here we review our recent effort along this direction, including (1) combining transmission electron microscopy and single-nanotube optical spectroscopy to establish an atlas for carbon nanotube optical transitions and (2) developing a high-contrast polarization microscope for real-time optical imaging and *in situ* spectroscopy of individual nanotubes in devices. We will also discuss the importance of such characterizations for controlled nanotube growth and for understanding chirality-dependent device behaviors. © 2016 Optical Society of America

OCIS codes: (140.3490) Lasers, distributed-feedback; (060.2420) Fibers, polarization-maintaining; (060.3735) Fiber Bragg gratings; (060.2370) Fiber optics sensors.

<http://dx.doi.org/10.1364/JOSAB.33.00C102>

1. INTRODUCTION

Since their discovery in 1991 [1], carbon nanotubes have revealed remarkable mechanical [2–6], thermal [7–9], electrical [10–14], and optical properties [15–22] and have been envisioned as the material of choice for numerous applications. With diameters on the order of 1 nm and lengths reaching centimeters, carbon nanotubes also constitute a model system for one-dimensional physics, a subject of long-standing experimental and theoretical interest [23–32].

A single-walled carbon nanotube can be viewed as rolled-up graphene sheet, and its structure is uniquely defined by the wrapping vector. The projection of the wrapping vector onto the graphene basis yields a two-coordinate number (n, m) , known as the chiral index of the nanotube [33,34]. Even with diameters smaller than 3 nm, there are hundreds of different nanotube species with different chiral indices. The electrical and optical properties of a nanotube depend sensitively on the precise tube structure, which can vary from semiconducting to metallic with the slightest change of chiral index [35,36]. This richness and diversity of carbon nanotubes make them appealing for a variety of very different applications [37–41]. To realize the potential of carbon nanotubes, we have to examine in detail the distinct physical behaviors of different nanotube species.

Single-nanotube spectroscopy provides a powerful tool for such studies [42–52]. Optical spectroscopy, with its non-invasive and noncontact nature, high spectral resolution, and superb sensitivity, has figured prominently in nanostructure research. Many optical techniques are sensitive enough to allow probing of individual carbon nanotubes, and single-nanotube spectroscopy has several distinct advantages. For a given individual nanotube, it has a well-defined chiral index, well-defined environment, and well-defined spatial location. Consequently, single-nanotube spectroscopy can yield a simplified spectrum with specific information, is capable of probing environmental effects, and can be readily combined with other characterization techniques.

This review mainly contains three parts. Part 1 introduces the nanotube's geometrical structure, tight-binding energy band structures, and many-body interactions, providing the background for discussing the optical transitions on carbon nanotubes. Part 2 presents the recent developments in establishing the atlas for carbon nanotube optical transitions and characterizing nanotubes in devices using single-nanotube spectroscopy. Part 3 discusses the applications of single-nanotube optical spectroscopy in chiral index feedback for nanotube growth and *in situ* study of nanotube device physics.

A. Background Knowledge about Carbon Nanotube Optical Transitions

The physical structure of single-walled carbon nanotubes can be regarded as rolled-up graphene and is uniquely defined by the circumferential chiral vector C_b as

$$C_b = na_1 + ma_2 = (n, m), \quad (1)$$

where a_1 and a_2 are the two basic vectors of a graphene unit cell [Fig. 1(a)]. The term (n, m) describes the chiral index or chirality of a nanotube [33,34]. The equivalent two parameters used to conveniently characterize nanotube structures are (d, θ) , i.e., diameter and chiral angle [relative angle between C_b and a_1 ; see Fig. 1(a)]. The diameter and chiral angle are related to (n, m) as in the relation

$$d = \frac{C_b}{\pi} = \sqrt{3}a_{cc}(m^2 + mn + n^2)^{1/2}/\pi, \quad (2)$$

$$\theta = \text{atan}\left(\frac{\sqrt{3}m}{2n + m}\right).$$

Here, a_{cc} is nearest-neighbor C–C distance.

The electronic band structures of carbon nanotubes can be analytically obtained from the tight-binding graphene band structures by the zone folding method [33,34]. Due to the finite circumference length, the momentum along the C_b direction is quantized into distinct states separated by $\Delta k = \frac{2\pi}{C_b} = \frac{2}{3d}$. Effectively, we can use a different “cutting line” to intersect with a two-dimensional graphene band structure and get a one-dimensional nanotube band structure. For $\text{mod}(n - m, 3) = 1, 2$ nanotubes, the smallest distance between the cutting line and the K point is $\frac{2}{3d}$ and they are semiconducting [Fig. 2(a)]; for $\text{mod}(n - m, 3) = 0$ nanotubes, one cutting line will go through the K point of the graphene Brillouin zone, and they are metallic [Fig. 2(b)]. Each cutting line will give one conduction band and one valence band, and at the minimum and maximum of these two bands, there exist van Hove singularities. The energy bandgap between the two singularities from the same cutting forms the subbandgap. Transitions at these bandgaps lead to strong optical resonances, and these transitions are called optical transitions, which are traditionally labeled S_{ii} for semiconducting and M_{ii} for metallic nanotubes [Figs. 2(c) and 2(d)], where i is the subband index. Mathematical calculations giving the distance from each cutting line to the K point can be simply described as $p \times 2/(3d)$, where p is an integer and has a value of 1, 2, 3,

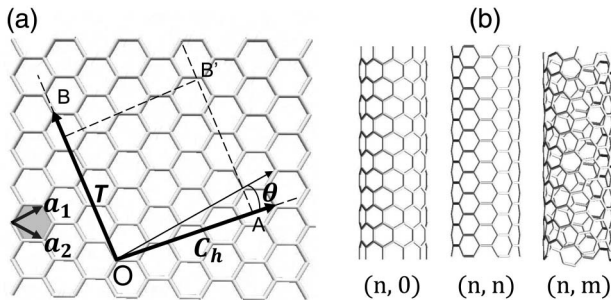


Fig. 1. Geometric structure of a carbon nanotube. (a) a_1 and a_2 are the two base vectors of the graphene lattice. C_b (T) is the circumferential (translational) chiral vector of a carbon nanotube. θ is the chiral angle. (b) Carbon nanotubes of different chiral indices.

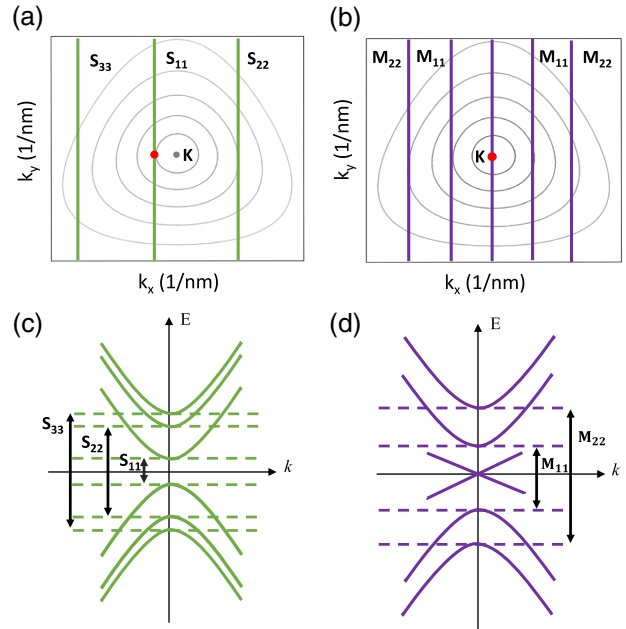


Fig. 2. Optical transitions in carbon nanotubes. (a), (b) Zone-folding pictures of (a) semiconducting and (b) metallic nanotubes. The contour curves are constant energy lines in the graphene Brillouin zone. The solid parallel lines describe available states consistent with the nanotube circumferential boundary condition. (c), (d) Illustration of (c) semiconducting and (d) metallic carbon nanotube optical transitions in E - k space.

4, 5, 6, 7, 8, 9, 10 ... for both semiconducting and metallic optical transitions in the order of $S_{11}, S_{22}, M_{11}, S_{33}, S_{44}, M_{22}, S_{55}, S_{66}, M_{33}, S_{77}, \dots$. Since the direction and distance to the K point from these cutting lines are solely determined by (n, m) , the optical transitions have a one-to-one correspondence to the chiral index. This correspondence forms the foundation for using an optical spectrum to determine the chiral index of carbon nanotubes, or to predict optical transitions of any given (n, m) nanotubes, if we can establish an accurate relationship between E_{ii} and (n, m) .

The optical transitions discussed above of carbon nanotube from the tight-binding method are based on a one-particle picture, where the many-body Coulomb interactions are ignored [53]. However, both experimental results and *ab initio* calculations based on GW approximation (expansion of the self-energy in terms of the Green function G and Coulomb interaction W) show that many-body effects could be prominent in the optical transition of carbon nanotubes [54–57]. In particular, the experimental peak positions can vary by hundreds of meV from the simple tight-binding predictions. Therefore, it is crucial to establish the one-to-one correspondence between the nanotube optical transitions and chiral structure experimentally.

2. RESULTS

A. Atlas for Carbon Nanotube Optical Transition Energy

As indicated above, the optical transitions of a carbon nanotube are directly related to its chiral index (n, m) . In real

experimental nanotubes, n or m can reach up to 35, and hence there exist more than 400 nanotube species. The nanotube community has long sought to establish a structure–property relation map for optical transitions in all these nanotube species.

We use Rayleigh scattering spectroscopy [19], which employs high-brightness supercontinuum white light on suspended nanotubes, to determine the optical resonances for individual nanotubes with an uncertainty of less than 20 meV. A significant source of this uncertainty is the difficult-to-control environmental effects, where unintentional mechanical strain, charge doping, and gas adsorption can shift the transition energy by ~ 10 meV. Complementarily, we use electron diffraction techniques in transmission electron microscopy (TEM) to determine the chiral index of the same nanotubes [58–60]. In this way the optical transitions and chiral index can be directly linked with each other [Figs. 3(a)–3(c)]. Previously only limited optical transitions in several nanotube species were studied in this combined way [46]. Recently, we studied more than 500 optical transitions from more than 200 nanotubes and established a complex and complete optical transitions–chiral index atlas [49].

With this experimental atlas, an experimental Katuara plot is then obtained [Fig. 3(d)], in which all dots are determined unambiguously by experiment data. Since this plot is based on experimental data, the accuracy reaches as high as 20 meV, compared to more than 100 meV for many nanotubes in previous plot [61]. This accurate Katuara plot forms the foundation for the future carbon nanotube studies and applications in nanoscale electronics, optoelectronics, and many-body interactions that utilize nanotubes of a specific chiral index. One note about this plot is that when we apply it on nanotubes

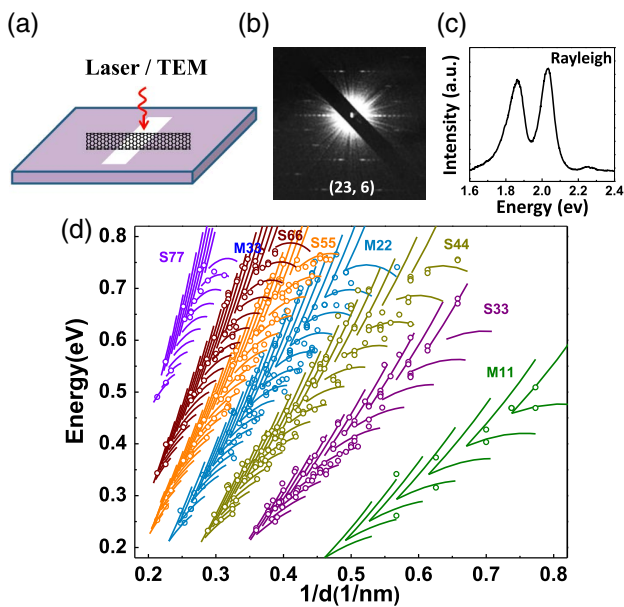


Fig. 3. Determination of carbon nanotube optical transition energy. (a) Schematic for combined TEM electron diffraction and Rayleigh scattering measurements on the same suspended nanotubes; (b), (c) electron diffraction pattern and Rayleigh scattering spectrum of the same suspended nanotube, respectively; (d) Katuara plot established experimentally by the combined TEM and Rayleigh scattering technique.

on substrates, the transition energies will be redshifted by about 40 meV due to the dielectric screening effects.

B. Quantitative Determination of Carbon Nanotube Absorption Cross Sections

Although Rayleigh scattering spectroscopy can efficiently determine the peak position of nanotube optical transitions, it does not yield the optical absolute absorption directly. Conventionally, optical absorption is widely used to characterize the linear optical properties of a material quantitatively. However, it is a great experimental challenge to measure the absorption in individual nanotubes, because the nanotube diameter is orders of magnitude smaller than the spot size of a focused laser beam [62,63].

Recently, a dramatic increase in the optical transmission contrast of individual carbon nanotubes has been successfully achieved by using a polarization-based homodyne technique, in which two polarizers were placed, respectively, at incoming and outgoing light paths with a relative angle of close to 90° with (δ deviation), and the nanotubes were put with their axis at 45° to the incoming polarizer [Fig. 5(a)] [50,64]. Under this geometry, the signal is enhanced by about 100 times, and thus becomes detectable by modern optical spectroscopic techniques. Using this method, quantitative determination of absorption cross sections was performed for more than 50 individual chirality-defined single-walled nanotubes (illustrated in Fig. 4). An empirical formula was established to describe the absorption cross section spectrum for any given nanotube [50]. The quantitative information of absorption cross sections in a broad spectral range and all nanotube species not only provides new insight into the unique photophysics in one-dimensional carbon nanotubes but also enables absolute determination of optical quantum efficiencies in important photoluminescence and photovoltaic processes.

C. Optical Spectroscopy of Individual Nanotubes in a Device

The atlas described above for nanotube optical transition energy and absorption cross sections is established based on single-nanotube optical spectroscopy on suspended nanotubes.

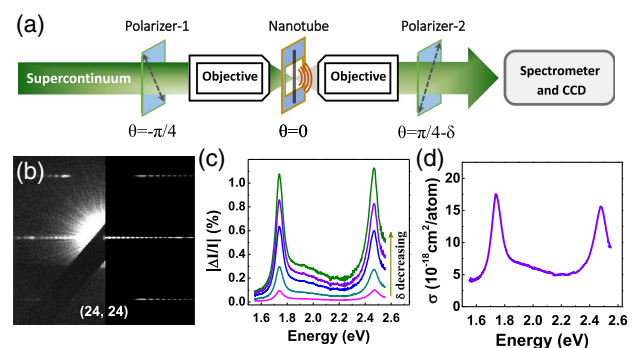


Fig. 4. Single-nanotube absorption cross section measurement with a defined chiral index. (a) Scheme of polarization-optimized homodyne detection for single-nanotube absorption, (b) electron diffraction patterns, (c) homodyne modulation signal ($\Delta I/I$) at various values of δ , and (d) absolute absorption cross section per carbon atom with parallel light polarization to nanotube axis.

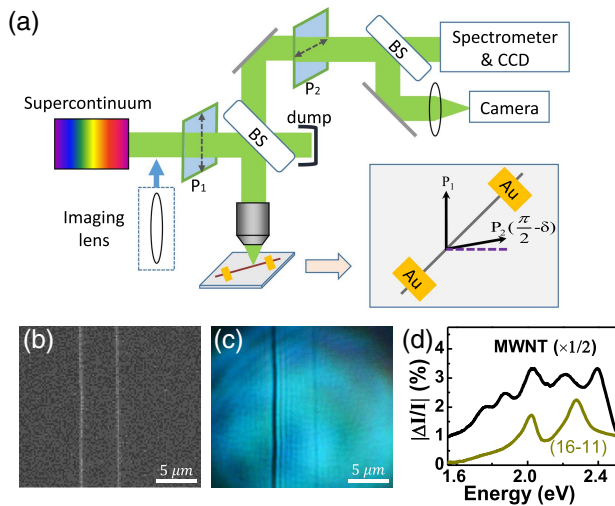


Fig. 5. Single-nanotube optical imaging and spectroscopy in the device. (a) Scheme for the combination of supercontinuum laser illumination and polarization-based high-contrast polarization microscopy for high-throughput individual nanotube imaging and chirality identification, (b) scanning electron microscopy images and (c) optical imaging and (d) *in situ* spectroscopy for a (16, 11) single-walled and a multi-walled nanotube (MWNT). BS: beam splitter.

For further study and real application in device physics and controlled growth, we need direct optical imaging and spectroscopy of nanotubes on substrates. Technically the background signal of nanotubes on growth substrates or in devices is more difficult to manipulate and control than that in suspended ones.

Recently we developed a polarization reflectance microscopy technique to address this problem [Fig. 5(a)] [52]. In our technique, we optimize the optical elements and the illumination/detection scheme with a supercontinuum light source to achieve an extinction ratio as high as 10^5 at a diffraction-limited spatial resolution. Horizontally polarized incident light (after polarizer 1) illuminates a nanotube oriented at 45° . The nanotube-scattered electrical field is polarized along the nanotube direction due to a strong depolarization effect on light polarized perpendicular to the nanotube, while the substrate reflection retains the horizontal polarization. Polarizer 2 is oriented close to the vertical direction (with δ deviation), which strongly reduces the substrate-reflected field by $\sin \delta$ but largely keeps the nanotube-scattered field. The nanotube contrast is therefore greatly enhanced. This technique enables high-throughput optical imaging [Fig. 5(c)] and *in situ* spectroscopy [Fig. 5(d)] on the substrate and in the device.

3. DISCUSSION

A. Chiral Index Feedback for Nanotube Growth

It is the holy grail in the nanotube field to achieve controlled growth of carbon nanotubes with a defined chiral index. Accurate and prompt feedback of the chirality distribution of as-grown nanotubes is crucial to realize this goal. The atlas

for carbon nanotube optical transitions, together with the direct optical imaging and *in situ* spectroscopy of carbon nanotubes on substrates, provides the platform for this chiral index feedback. By this method, the detailed chirality distribution of hundreds of nanotubes on as-grown substrates (transparent or opaque) can be determined accurately [Fig. 6(a)]. The chirality [Fig. 6(b)], diameter [Fig. 6(c)], and chiral angle distribution [Fig. 6(d)] all show that different kinds of nanotubes are enriched in different regions [52]. This quick feedback is critical to accelerating the controllable growth of carbon nanotubes. Recent study using this technique further shows that by controlling the carbon sources, the richness ratio between metallic and semiconducting nanotubes can be controlled in a certain range [65,66].

B. In situ Study of Nanotube Device Physics

Future nanotube device applications surely rely on the full understanding of their device physics under operating conditions. *In situ* imaging and spectroscopy of individual nanotubes in devices offer new opportunities to probe nanotube physics in operating devices. As an example, gate-variable nanotube optical transitions in field-effect devices were measured to investigate electron–electron interaction effects on excited states in nanotubes [52]. Optical spectra for a (27, 18) metallic nanotube show significant broadening, with the gate voltage varying from close to 20 V to -20 V [Fig. 7(a)]. This broadening indicates a new type of electron–electron interaction. Figures 7(b) and 7(c) show the representative scattering channels that satisfy the stringent conservation requirements of energy, momentum, and angular momentum by the quantum number E , k , and μ respectively. Such scattering between optically excited electrons and free holes (in another valley) is absent in pristine undoped carbon nanotubes [Fig. 7(b)], but emerges with hole doping [Fig. 7(c)].

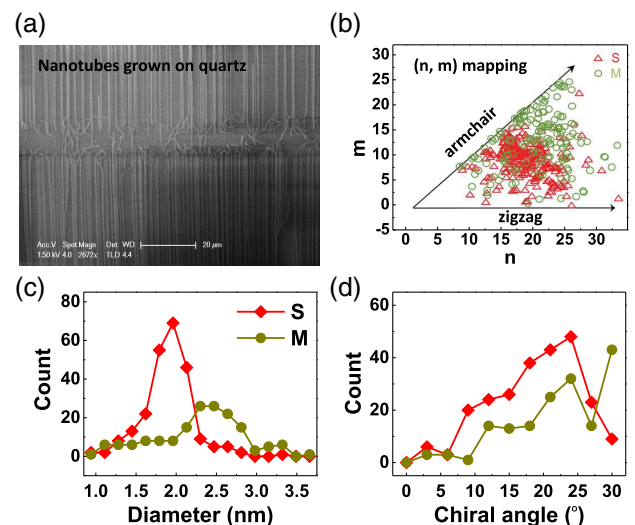


Fig. 6. High-throughput chirality profiling of 402 single-walled carbon nanotubes from one growth condition. (a) The scanning electron microscopic image of nanotube sample grown on quartz and (b)–(d) chirality, diameter, and chiral angle distribution, respectively, of semiconducting and metallic nanotubes, showing inhomogeneous enrichment.

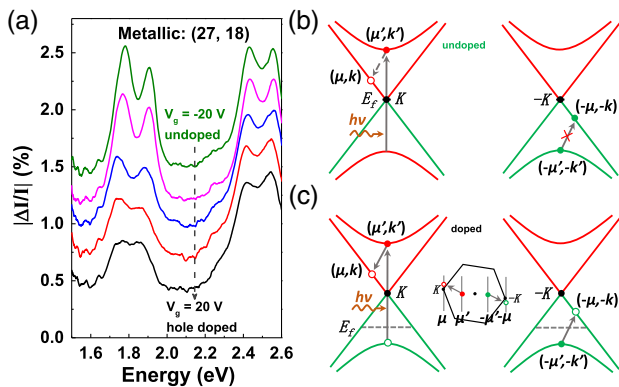


Fig. 7. Gate-variable nanotube optical transitions in field-effect devices. (a) Optical spectral evolution of metallic (27, 18) nanotube under different back-gated voltages. $V_g \sim -20$ – 20 V, which corresponds to the change from the undoped state to the hole doping of $\sim 0.45e$ nm $^{-1}$. (b), (c) Schematic illustration of one representative ultrafast decay pathway of an optically excited electron due to intersubband electron–electron scattering in doped metallic nanotubes.

4. SUMMARY

In this review we have discussed optical spectroscopy and imaging of individual carbon nanotubes, based on which an atlas of carbon nanotube optical transition energy and absorption cross section with a defined index was built up and the *in situ* study of carbon nanotubes in devices and on substrates has been realized. These techniques can enable new directions in nanotube research, for example, for realizing *in situ* optical monitoring of nanotube growth for chirality control and exploring chirality-dependent nonlinear optical response in carbon nanotubes. We believe such development will lead to further understanding of nanotube physics and contribute to its application in nanotechnology.

Funding. National Science Foundation (NSF) (DMR-1404865); National Natural Science Foundation of China (NSFC) (51522201, 11474006, 91433102).

REFERENCES

- S. Iijima, "Helical microtubules of graphitic carbon," *Nature* **354**, 56–58 (1991).
- M. M. J. Treacy, T. W. Ebbesen, and J. M. Gibson, "Exceptionally high Young's modulus observed for individual carbon nanotubes," *Nature* **381**, 678–680 (1996).
- M. R. Falvo, G. J. Clary, R. M. Taylor, V. Chi, F. P. Brooks, S. Washburn, and R. Superfine, "Bending and buckling of carbon nanotubes under large strain," *Nature* **389**, 582–584 (1997).
- P. Poncharal, Z. L. Wang, D. Ugarte, and W. A. de Heer, "Electrostatic deflections and electromechanical resonances of carbon nanotubes," *Science* **283**, 1513–1516 (1999).
- S. B. Cronin, A. K. Swan, M. S. Unlu, B. B. Goldberg, M. S. Dresselhaus, and M. Tinkham, "Measuring the uniaxial strain of individual single-wall carbon nanotubes: resonance Raman spectra of atomic-force-microscope modified single-wall nanotubes," *Phys. Rev. Lett.* **93**, 167401 (2004).
- Y. Wu, M. Y. Huang, F. Wang, X. M. H. Huang, S. Rosenblatt, L. M. Huang, H. G. Yan, S. P. O'Brien, J. Hone, and T. F. Heinz, "Determination of the Young's modulus of structurally defined carbon nanotubes," *Nano Lett.* **8**, 4158–4161 (2008).

- P. Kim, L. Shi, A. Majumdar, and P. L. McEuen, "Thermal transport measurements of individual multiwalled nanotubes," *Phys. Rev. Lett.* **87**, 215502 (2001).
- D. G. Cahill, W. K. Ford, K. E. Goodson, G. D. Mahan, A. Majumdar, H. J. Maris, R. Merlin, and S. R. Phillpot, "Nanoscale thermal transport," *J. Appl. Phys.* **93**, 793–818 (2003).
- A. Majumdar, "Thermoelectricity in semiconductor nanostructures," *Science* **303**, 777–778 (2004).
- H. J. Dai, E. W. Wong, and C. M. Lieber, "Probing electrical transport in nanomaterials: conductivity of individual carbon nanotubes," *Science* **272**, 523–526 (1996).
- T. W. Ebbesen, H. J. Lezec, H. Hiura, J. W. Bennett, H. F. Ghaemi, and T. Thio, "Electrical conductivity of individual carbon nanotubes," *Nature* **382**, 54–56 (1996).
- L. Langer, V. Bayot, E. Grivei, J. P. Issi, J. P. Heremans, C. H. Olk, L. Stockman, C. Van Haesendonck, and Y. Bruynseraede, "Quantum transport in a multiwalled carbon nanotube," *Phys. Rev. Lett.* **76**, 479–482 (1996).
- M. Bockrath, D. H. Cobden, P. L. McEuen, N. G. Chopra, A. Zettl, A. Thess, and R. E. Smalley, "Single-electron transport in ropes of carbon nanotubes," *Science* **275**, 1922–1925 (1997).
- A. Javey, J. Guo, Q. Wang, M. Lundstrom, and H. J. Dai, "Ballistic carbon nanotube field-effect transistors," *Nature* **424**, 654–657 (2003).
- A. M. Rao, E. Richter, S. Bandow, B. Chase, P. C. Eklund, K. A. Williams, S. Fang, K. R. Subbaswamy, M. Menon, A. Thess, R. E. Smalley, G. Dresselhaus, and M. S. Dresselhaus, "Diameter-selective Raman scattering from vibrational modes in carbon nanotubes," *Science* **275**, 187–191 (1997).
- S. M. Bachilo, M. S. Strano, C. Kittrell, R. H. Hauge, R. E. Smalley, and R. B. Weisman, "Structure-assigned optical spectra of single-walled carbon nanotubes," *Science* **298**, 2361–2366 (2002).
- M. J. O'Connell, S. M. Bachilo, C. B. Huffman, V. C. Moore, M. S. Strano, E. H. Haroz, K. L. Rialon, P. J. Boul, W. H. Noon, C. Kittrell, J. P. Ma, R. H. Hauge, R. B. Weisman, and R. E. Smalley, "Band gap fluorescence from individual single-walled carbon nanotubes," *Science* **297**, 593–596 (2002).
- C. D. Spataru, S. Ismail-Beigi, L. X. Benedict, and S. G. Louie, "Excitonic effects and optical spectra of single-walled carbon nanotubes," *Phys. Rev. Lett.* **92**, 077402 (2004).
- M. Y. Sfeir, F. Wang, L. M. Huang, C. C. Chuang, J. Hone, S. P. O'Brien, T. F. Heinz, and L. E. Brus, "Probing electronic transitions in individual carbon nanotubes by Rayleigh scattering," *Science* **306**, 1540–1543 (2004).
- J. C. Meyer, M. Paillet, T. Michel, A. Moreac, A. Neumann, G. S. Duesberg, S. Roth, and J. L. Sauvajol, "Raman modes of index-identified freestanding single-walled carbon nanotubes," *Phys. Rev. Lett.* **95**, 217401 (2005).
- F. Wang, G. Dukovic, L. E. Brus, and T. F. Heinz, "The optical resonances in carbon nanotubes arise from excitons," *Science* **308**, 838–841 (2005).
- F. Wang, W. T. Liu, Y. Wu, M. Y. Sfeir, L. M. Huang, J. Hone, S. O'Brien, L. E. Brus, T. F. Heinz, and Y. R. Shen, "Multiphonon Raman scattering from individual single-walled carbon nanotubes," *Phys. Rev. Lett.* **98**, 047402 (2007).
- H. Ajiki and T. Ando, "Aharonov-Bohm effect in carbon nanotubes," *Physica B* **201**, 349–352 (1994).
- S. J. Tans, M. H. Devoret, H. J. Dai, A. Thess, R. E. Smalley, L. J. Geerlings, and C. Dekker, "Individual single-wall carbon nanotubes as quantum wires," *Nature* **386**, 474–477 (1997).
- M. Bockrath, D. H. Cobden, J. Lu, A. G. Rinzler, R. E. Smalley, L. Balents, and P. L. McEuen, "Luttinger-liquid behaviour in carbon nanotubes," *Nature* **397**, 598–601 (1999).
- J. Nygard, D. H. Cobden, and P. E. Lindelof, "Kondo physics in carbon nanotubes," *Nature* **408**, 342–346 (2000).
- H. W. C. Postma, T. Teepen, Z. Yao, M. Grifoni, and C. Dekker, "Carbon nanotube single-electron transistors at room temperature," *Science* **293**, 76–79 (2001).
- H. Ishii, H. Kataura, H. Shiozawa, H. Yoshioka, H. Otsubo, Y. Takayama, T. Miyahara, S. Suzuki, Y. Achiba, M. Nakatake, T. Narimura, M. Higashiguchi, K. Shimada, H. Namatame, and M.

- Taniguchi, "Direct observation of Tomonaga-Luttinger-liquid state in carbon nanotubes at low temperatures," *Nature* **426**, 540–544 (2003).
29. M. F. Islam, D. E. Milkie, C. L. Kane, A. G. Yodh, and J. M. Kikkawa, "Direct measurement of the polarized optical absorption cross section of single-wall carbon nanotubes," *Phys. Rev. Lett.* **93**, 037404 (2004).
 30. V. V. Deshpande, M. Bockrath, L. I. Glazman, and A. Yacoby, "Electron liquids and solids in one dimension," *Nature* **464**, 209–216 (2010).
 31. S. M. Santos, B. Yuma, S. Berciaud, J. Shaver, M. Gallart, P. Gilliot, L. Cognet, and B. Lounis, "All-optical trion generation in single-walled carbon nanotubes," *Phys. Rev. Lett.* **107**, 187401 (2011).
 32. Z. W. Shi, X. P. Hong, H. A. Bechtel, B. Zeng, M. C. Martin, K. Watanabe, T. Taniguchi, Y. R. Shen, and F. Wang, "Observation of a Luttinger-liquid plasmon in metallic single-walled carbon nanotubes," *Nat. Photonics* **9**, 515–519 (2015).
 33. R. Saito, G. Dresselhaus, and M. S. Dresselhaus, *Physical Properties of Carbon Nanotubes* (Imperial College, 1998).
 34. S. Reich, C. Thomsen, and J. Maultzsch, *Carbon Nanotubes: Basic Concepts and Physical Properties* (Wiley-VCH, 2004).
 35. T. W. Odom, J. L. Huang, P. Kim, and C. M. Lieber, "Atomic structure and electronic properties of single-walled carbon nanotubes," *Nature* **391**, 62–64 (1998).
 36. J. W. G. Wildoer, L. C. Venema, A. G. Rinzler, R. E. Smalley, and C. Dekker, "Electronic structure of atomically resolved carbon nanotubes," *Nature* **391**, 59–62 (1998).
 37. P. Avouris, Z. H. Chen, and V. Perebeinos, "Carbon-based electronics," *Nat. Nanotechnol.* **2**, 605–615 (2007).
 38. P. Avouris, M. Freitag, and V. Perebeinos, "Carbon-nanotube photonics and optoelectronics," *Nat. Photonics* **2**, 341–350 (2008).
 39. T. Hertel, "Carbon nanotubes: a brighter future," *Nat. Photonics* **4**, 77–78 (2010).
 40. A. D. Franklin, "Electronics: the road to carbon nanotube transistors," *Nature* **498**, 443–444 (2013).
 41. M. M. Shulaker, G. Hills, N. Patil, H. Wei, H.-Y. Chen, H. S. Philip Wong, and S. Mitra, "Carbon nanotube computer," *Nature* **501**, 526–530 (2013).
 42. A. Hartschuh, H. N. Pedrosa, L. Novotny, and T. D. Krauss, "Simultaneous fluorescence and Raman scattering from single carbon nanotubes," *Science* **301**, 1354–1356 (2003).
 43. J. Lefebvre, Y. Homma, and P. Finnie, "Bright band gap photoluminescence from unprocessed single-walled carbon nanotubes," *Phys. Rev. Lett.* **90**, 217401 (2003).
 44. H. Telg, J. Maultzsch, S. Reich, F. Hennrich, and C. Thomsen, "Chirality distribution and transition energies of carbon nanotubes," *Phys. Rev. Lett.* **93**, 177401 (2004).
 45. C. Fantini, A. Jorio, M. Souza, M. S. Strano, M. S. Dresselhaus, and M. A. Pimenta, "Optical transition energies for carbon nanotubes from resonant Raman spectroscopy: environment and temperature effects," *Phys. Rev. Lett.* **93**, 147406 (2004).
 46. M. Y. Sfeir, T. Beetz, F. Wang, L. M. Huang, X. M. H. Huang, M. Y. Huang, J. Hone, S. O'Brien, J. A. Misewich, T. F. Heinz, L. J. Wu, Y. M. Zhu, and L. E. Brus, "Optical spectroscopy of individual single-walled carbon nanotubes of defined chiral structure," *Science* **312**, 554–556 (2006).
 47. F. Wang, M. Y. Sfeir, L. M. Huang, X. M. H. Huang, Y. Wu, J. H. Kim, J. Hone, S. O'Brien, L. E. Brus, and T. F. Heinz, "Interactions between individual carbon nanotubes studied by Rayleigh scattering spectroscopy," *Phys. Rev. Lett.* **96**, 167401 (2006).
 48. D. Y. Joh, L. H. Herman, S.-Y. Ju, J. Kinder, M. A. Segal, J. N. Johnson, G. K. L. Chan, and J. Park, "On-chip Rayleigh imaging and spectroscopy of carbon nanotubes," *Nano Lett.* **11**, 1–7 (2011).
 49. K. Liu, J. Deslippe, F. Xiao, R. B. Capaz, X. Hong, S. Aloni, A. Zettl, W. Wang, X. Bai, S. G. Louie, E. Wang, and F. Wang, "An atlas of carbon nanotube optical transitions," *Nat. Nanotechnol.* **7**, 325–329 (2012).
 50. K. H. Liu, X. P. Hong, S. Choi, C. H. Jin, R. B. Capaz, J. Kim, W. L. Wang, X. D. Bai, S. G. Louie, E. G. Wang, and F. Wang, "Systematic determination of absolute absorption cross-section of individual carbon nanotubes," *Proc. Natl. Acad. Sci.* **111**, 7564–7569 (2014).
 51. D. Y. Joh, J. Kinder, L. H. Herman, S. Y. Ju, M. A. Segal, J. N. Johnson, G. K. L. Chan, and J. Park, "Single-walled carbon nanotubes as excitonic optical wires," *Nat. Nanotechnol.* **6**, 51–56 (2011).
 52. K. Liu, X. Hong, Q. Zhou, C. Jin, J. Li, W. Zhou, J. Liu, E. Wang, A. Zettl, and F. Wang, "High-throughput optical imaging and spectroscopy of individual carbon nanotubes in devices," *Nat. Nanotechnol.* **8**, 917–922 (2013).
 53. T. Ando, "Excitons in carbon nanotubes," *J. Phys. Soc. Jpn.* **66**, 1066–1073 (1997).
 54. C. L. Kane and E. J. Mele, "Electron interactions and scaling relations for optical excitations in carbon nanotubes," *Phys. Rev. Lett.* **93**, 197402 (2004).
 55. V. Perebeinos, J. Tersoff, and P. Avouris, "Scaling of excitons in carbon nanotubes," *Phys. Rev. Lett.* **92**, 257402 (2004).
 56. H. B. Zhao and S. Mazumdar, "Electron-electron interaction effects on the optical excitations of semiconducting single-walled carbon nanotubes," *Phys. Rev. Lett.* **93**, 157402 (2004).
 57. F. Wang, D. J. Cho, B. Kessler, J. Deslippe, P. J. Schuck, S. G. Louie, A. Zettl, T. F. Heinz, and Y. R. Shen, "Observation of excitons in one-dimensional metallic single-walled carbon nanotubes," *Phys. Rev. Lett.* **99**, 227401 (2007).
 58. Z. L. Wang, P. Poncharal, and W. A. de Heer, "Measuring physical and mechanical properties of individual carbon nanotubes by in situ TEM," *J. Phys. Chem. Solids* **61**, 1025–1030 (2000).
 59. Z. J. Liu and L. C. Qin, "A direct method to determine the chiral indices of carbon nanotubes," *Chem. Phys. Lett.* **408**, 75–79 (2005).
 60. K. H. Liu, Z. Xu, W. L. Wang, P. Gao, W. Y. Fu, X. D. Bai, and E. G. Wang, "Direct determination of atomic structure of large-indexed carbon nanotubes by electron diffraction: application to double-walled nanotubes," *J. Phys. D* **42**, 125412 (2009).
 61. P. T. Araujo, S. K. Doorn, S. Kilina, S. Tretiak, E. Einarsson, S. Maruyama, H. Chacham, M. A. Pimenta, and A. Jorio, "Third and fourth optical transitions in semiconducting carbon nanotubes," *Phys. Rev. Lett.* **98**, 067401 (2007).
 62. F. Violla, C. Roquelet, B. Langlois, G. Delport, S. M. Santos, E. Deleporte, P. Roussignol, C. Delalande, C. Voisin, and J.-S. Lauret, "Chirality dependence of the absorption cross section of carbon nanotubes," *Phys. Rev. Lett.* **111**, 137402 (2013).
 63. J.-C. Blancon, M. Paillet, H. N. Tran, X. T. Than, S. A. Guebrou, A. Ayari, A. S. Miguel, N.-M. Phan, A.-A. Zahab, J.-L. Sauvajol, N. D. Fatti, and F. Vallée, "Direct measurement of the absolute absorption spectrum of individual semiconducting single-wall carbon nanotubes," *Nat. Commun.* **4**, 2542 (2013).
 64. J. Lefebvre and P. Finnie, "Polarized light microscopy and spectroscopy of individual single-walled carbon nanotubes," *Nano Res.* **4**, 788–794 (2011).
 65. J. H. Li, C. T. Ke, K. H. Liu, P. Li, S. H. Liang, G. Finkelstein, F. Wang, and J. Liu, "Importance of diameter control on selective synthesis of semiconducting single-walled carbon nanotubes," *ACS Nano* **8**, 8564–8572 (2014).
 66. J. H. Li, K. H. Liu, S. B. Liang, W. W. Zhou, M. Pierce, F. Wang, L. M. Peng, and J. Liu, "Growth of high-density-aligned and semiconducting-enriched single-walled carbon nanotubes: decoupling the conflict between density and selectivity," *ACS Nano* **8**, 554–562 (2014).